COLLOID CHEMICAL ASPECTS OF CORROSION OF METALS

Egon Matijević

Institute of Colloid and Surface Science, Clarkson College of Technology,
Potsdam, New York, 13676 U.S.A.

Abstract - The corrosion of metals and alloys results in the formation of
soluble hydroxylated complexes and precipitated metal hydrous oxides,
with the end-products almost invariably in colloidal state as films,
particles, or particle aggregates. It is, therefore, obvious that in the
course of the corrosion process the materials undergo chemical and mor-
phological changes. Even if precipitation does not occur, the solution
adjacent to the metal surface will have an entirely different composition
than the bulk liquid phase.
   Little *proven* information is available on the chemical mechanism of
the processes involved in the precipitation of metal (hydrous) oxides.
This is, in part, due to the complexity of reactions involved in the
solid phase formation and to the sensitivity of precipitation processes
to various parameters, making it difficult to reproduce a given material.
   Recently, it was possible to develop well defined colloidal metal
hydrous oxides which can serve as models for corrosion products. These
systems consist of particles uniform in chemical composition, size, and
shape, that can be repeatedly generated under reproducible conditions.
The so prepared "monodispersed" sols are used to elucidate the chemical
mechanism of metal corrosion processes, to study the properties of the
model corrosion products (surface, electric, magnetic, optical, etc.),
to investigate their interactions with various additives (chelating
agents, etc.), and, finally, to establish factors governing their ad-
hesion or the detachment from different substrates.
   Examples of these model dispersions are shown and various studies,
relevant to corrosion of metals in general and of iron in particular,
carried out with such materials are discussed.

INTRODUCTION

   The problems of corrosion of metals are usually associated with electrochemical and
material sciences. The experts in these fields have made significant contributions towards
the understanding of the scientifically interesting phenomena involved in corrosion. In
many instances they have found ways in preventing or, at least, retarding the deterioration
of metal surfaces. Needless to say, the latter achievements are of enormous economic sig-
nificance.
   Surprisingly, relatively few colloid and interface scientists have dealt in depth with
the various processes related to corrosion of metals. Yet, it can be easily recognized
that the colloid discipline should play a critical role in this technologically important
area. The origin of most corrosion phenomena involving metals is at the interface
between the solid and a solution. The nature of the products of these interfacial reactions
are dependent on the local solute concentrations, which may greatly differ from those in the
bulk. Thus, in metal corrosion solute complexations must be regarded as surface processes.
The hydrolysis of metal ions, originating from the solid matrix, and their interactions
with anions take place under a regime which is entirely different than the regime in the
same system farther away from the interfacial region. Parameters in addition to ionic
strength and pH (dielectric constant, ion hydration, viscosity, etc.) cannot be assumed to
be the same as in the continuous phase.
   The interfacial metal complexes act as precursors to nuclei formation. They are also the
determining factor in the subsequent growth of the corrosion products - various metal
(hydrous) oxides. The solid phase so produced may result either in a film or in matter of
different particle sizes, shapes, chemical composition, and degrees of aggregation. For a
given metal, the nature of the formed layer will be exceedingly sensitive to pH, tempera-
ture, ionic strength, and the anions present. The latter may not even appear in the final
solids, but still influence their physical and chemical characteristics. The originally
formed corrosion products frequently undergo changes on aging, which may be compositional
or morphological transformations, or both.
   Depending on the local conditions, the metal (hydrous) oxides adhere to the surface or
they may detach from the substrate, frequently yielding colloidal dispersions. The sta-

bility of these finely divided systems towards aggregation depends on the charge, hydration, and other properties of the dispersed material as well as on the composition of the liquid environment. The sol stability is in itself a classical area of concern of colloid science.

The suspended particles often redeposit on various surfaces, particularly in circulating systems. The adhesion of colloids on solid substrates and their removal from such surfaces is subject to the same type of forces, physical and chemical, as must be considered in particle/particle interactions.

The addition of various solutes, such as chelating agents, as inhibitors or decontaminants again require the knowledge of interfacial processes which may lead to surface stabilization or dissolution phenomena.

In order to develop an understanding of different mechanisms of corrosion, which may be operative under specific conditions, it is necessary to reproducibly prepare metal (hydrous) oxides in a manner that simulates crud formation under different realistic situations. Furthermore, it is essential that all solute complexes be known during all stages of precipitation. Unfortunately, only limited thermodynamic data on the pertinent solute metal species (particularly at elevated temperature) are available.

The difficult task of explaining various phenomena of metal corrosion would be greatly facilitated if well defined colloidal metal (hydrous) oxide systems could be generated to serve as model systems. Using several different techniques we have succeeded in this effort and now a number of dispersions of varying chemical composition, consisting of particles exceedingly uniform in size and shape have been obtained. Of special interest is that some of these systems contain monodispersed spheres, making it possible to quantitatively interpret a variety of the observed phenomena. In a number of cases the composition of the species in solutions from which such uniform particles precipitated were also ascertained. This information allowed for the elucidation of the chemical mechanism of metal (hydrous) oxide formation under the exact conditions of the experiments.

The model corrosion products are also used to study their properties (electric, magnetic, optical, etc.) and to elucidate their interactions with different solutes and other particles or substrates. The purpose of this lecture is to illustrate some of the novel results in this fascinating field of research.

PREPARATION OF THE MODEL COLLOIDAL CORROSION PRODUCTS

The processes involved in the corrosion of metals and the nature of the final corrosion products greatly depend on the conditions of the environment in which the metals are located. Thus, it is highly desirable to produce model systems in a variety of ways that are representative of different situations. Three such procedures will be described in this work.

A. Forced Hydrolysis

Most metal ions, particularly the polyvalent ones, readily hydrolyze. The rate of hydroxylation strongly depends on the pH and temperature; on heating, the deprotonation of the hydrated metal ions may take place even in highly acidic solutions. If hydrolysis proceeds far enough one or more metal (hydrous) oxides precipitate. The final product will be also affected by the anions present in the solution.

In corrosion of metals, ions of different oxidation states are generated, which further react to yield metal oxides and/or hydroxides. For example, it is well known that the corrosion products of iron and steel greatly differ when formed in marine, industrial, or rural atmospheres. Specifically, SO_2 in polluted air accelerates the rust formation, which is even more pronounced under humid conditions. Since SO_2 is readily oxidized on iron surfaces to SO_3, the corrosion of iron under these conditions must involve reactions of ferric ions in sulfuric acid solutions. In an atmosphere rich in chloride ions, any corrosion of metals will be influenced by the presence of hydrochloric acid.

Two examples are offered to show that uniform particles can be obtained by forced hydrolysis at elevated temperature of highly acidified solutions of ferric salts. Figure 1 and 2 are scanning electron micrographs of a basic ferric sulfate (Refs. 1 & 2) and of a hematite dispersion (Ref. 3), respectively, prepared under the conditions given in the legends. Both kinds of particles give pronounced X-ray patterns. Whereas the basic ferric sulfate, $Fe_3(OH)_5(SO_4)_2$, (Fig. 1) appears in the form of well defined crystals, $\alpha\text{-}Fe_2O_3$ (Fig. 2) consists of spheres of narrow size distribution. By changing the experimental conditions, hematite particles of other morphologies can be obtained, yet in all cases hydrochloric acid is present in the aging solution. It is important to note that the submicronic crystals precipitated in the ferric salt solutions containing sulfuric acid have the sulfate group incorporated as constituent species of stoichiometric composition. Particles formed in hydrochloric acid solutions contain chloride ions, but these are readily removed by leaching with water.

Using analogous techniques, it has been possible to prepare a number of "monodispersed" (hydrous) oxide sols of aluminum (Ref. 4), chromium (Refs. 5 & 6), titanium (Ref. 7), and copper (Ref. 8).
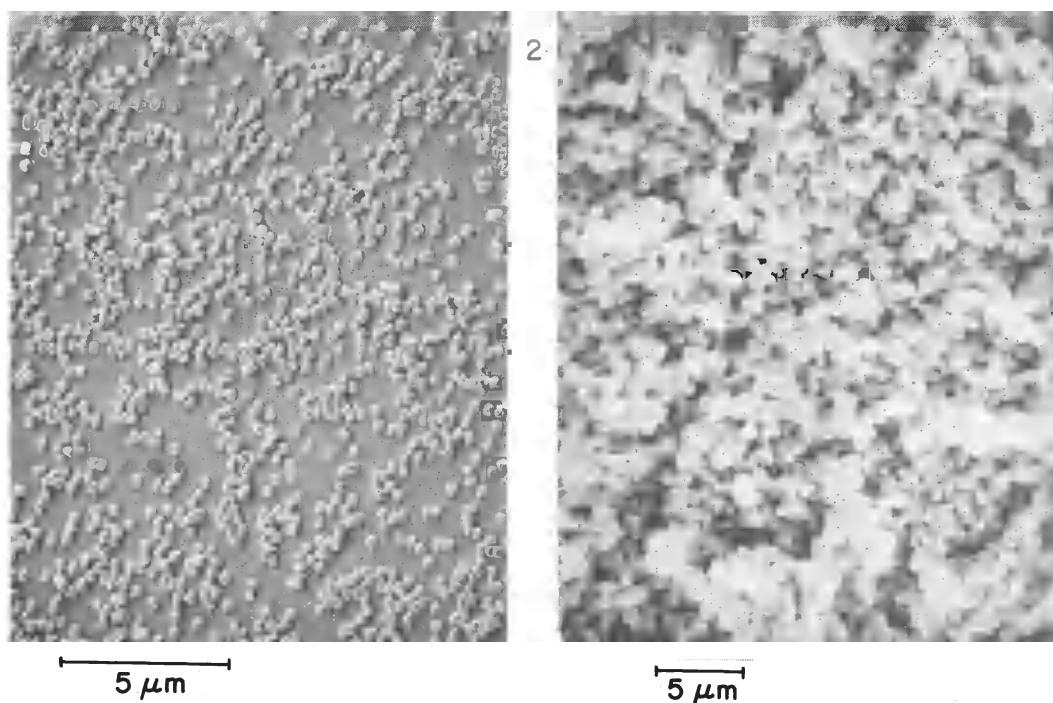
Fig. 1.   Scanning electron micrograph of ferric basic sulfate particles obtained by aging for 0.5 hr at 80°C a solution 0.18 M in Fe(NO$_3$)$_3$ and 0.53 M in Na$_2$SO$_4$.

Fig. 2.   Scanning electron micrograph of hematite (α-Fe$_2$O$_3$) particles obtained by aging for 10 days at 100°C a solution 0.032 M in FeCl$_3$ and 0.005 M in HCl.
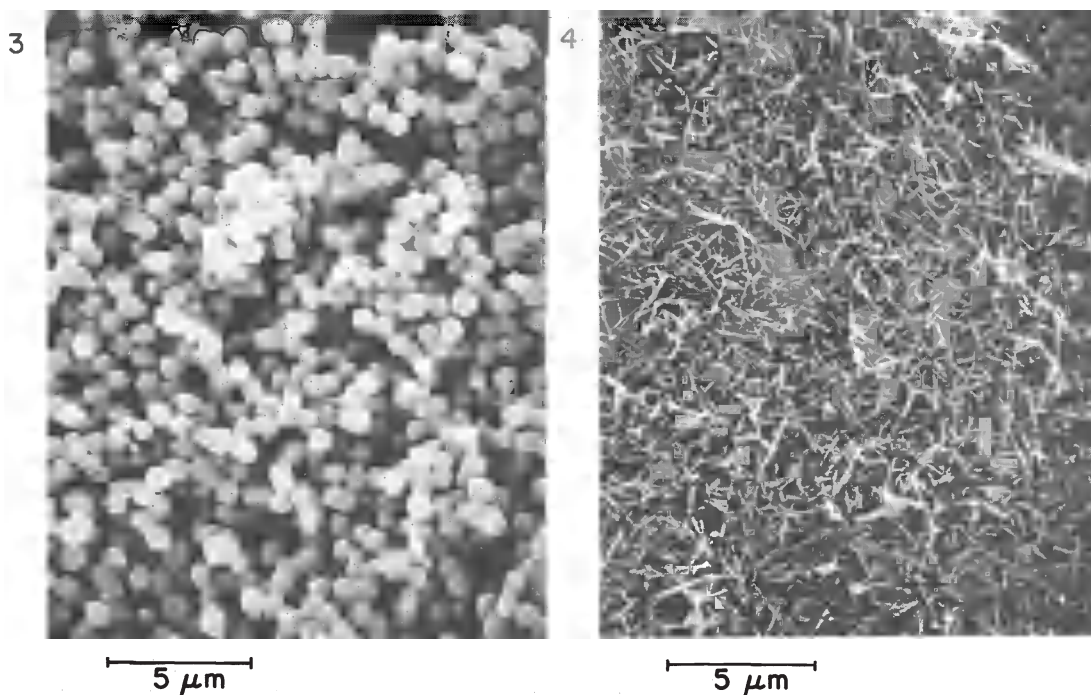

Fig. 3.   Scanning electron micrograph of magnetite (Fe$_3$O$_4$) particles obtained by aging for 4 hr at 90°C a ferrous hydroxide gel (0.025 M) containing 0.2 M KNO$_3$ and 0.005 M excess concentration of FeSO$_4$.

Fig. 4.   Scanning electron micrograph of goethite (α-FeOOH) particles obtained by aging for 4 hr at 90°C a ferrous hydroxide gel (0.2 M) containing 0.2 M KNO$_3$ and 0.01 M excess concentration of FeSO$_4$ in the presence of air. The particles were separated from magnetite spheres co-precipitated under the same conditions.

B. Crystallization from Gels

The precipitation of metal (hydrous) oxide particles may be preceded by the formation of a hydroxide gel of the same metal and subsequent crystallization on aging. Indeed, it has been suggested that in certain corrosion processes a gelatinous film is first generated on the metal surface, which then may change into a crystalline phase.

Again it was possible to produce well defined colloidal dispersions by crystallization from gels. Figure 3 shows magnetite (Fe_3O_4) particles which were obtained by aging at 90°C in an inert atmosphere a ferrous hydroxide gel in the presence of KNO_3 and excess $FeSO_4$ (Ref. 9). This example seems to represent the first colloidal magnetite of spherical morphology and of narrow size distribution ever reported in the literature. The average size of the particles can be altered by varying the amount of $FeSO_4$ in the gel. When the base is in excess, magnetite appears in the form of cubic particles.

If the aging of the ferrous hydroxide gel is carried out in air, the stronger oxidation environment produces, under certain conditions, a mixture of magnetite and goethite (α-FeOOH). Each of these solids appears in entirely different morphology. The spherical magnetite, Fe_3O_4, can be readily removed by density sedimentation aided by a magnetic field; the remaining goethite consists of uniform rod-like particles as shown in Fig. 4.

C. Decomposition of Solute Metal Complexes

The addition of complexing agents, and particularly of molecules capable of chelating metal ions, is common either in corrosion inhibition or in decontamination of water cooled nuclear reactors. Under certain conditions, these additives may enhance corrosion, or cause the formation of unusual corrosion products.

Again, it was possible to show that the decomposition of metal chelates may indeed yield metal (hydrous) oxides of rather unique particle morphologies. Figure 5 exemplifies such a system consisting of disc-like hematite particles; the solid was formed on aging in an autoclave at 250°C for 1 hr a ferric perchlorate solution in the presence of triethanolamine (TEA), H_2O_2 and NaOH.

The advantage of the described method for the preparation of metal hydrous oxide dispersions is that the conditions can be widely altered by additives (oxidizing or reducing agents, different electrolytes, etc.) which can yield a variety of products. For example, the presence of sodium acetate in a system similar to that described in Fig. 5 yields rather uniform hexagonal platelets of hematite (Fig. 6). If a reducing agent is added (such as hydrazine), magnetite particles are formed instead (Ref. 10).

The same procedure was used with chelates of nickel, cobalt, copper, vanadium, and bismuth and unique dispersions of metals and metal oxides were obtained. Figure 7 illustrates rather unusual copper oxide particles generated by aging at 100°C for 1 hr a copper(II) nitrate solution to which HEDTA and NaOH were added.

D. Phase Transformation

In addition to crystallization in gels (described in section B) it is possible to show that phase transformations of well defined systems can occur if the experimental conditions are suitably adjusted.

The scanning electron micrograph (Fig. 8) clearly shows a partial recrystallization of spherical hematite particles (the preparation of which was described in section A) into octahedral magnetite crystals (Ref. 10). The phase transformation was accomplished by heating the hematite sol in the presence of hydrazine and NaOH at 250°C. On longer aging all the αFe_2O_3 particles are converted to magnetite. It was established that the phase transformation proceeds through dissolution of the original hematite particles and subsequent crystallization of magnetite.

CHARACTERIZATION AND PROPERTIES

The monodispersed sols of metal (hydrous) oxides lend themselves well for the studies of various particle and dispersion properties. The information so obtained is of importance in explaining different corrosion phenomena or in technological applications related to corrosion processes. Some examples of magnetic, electrokinetic, optical, and stability characteristics are given below.

A. Magnetic Properties

One of the intriguing aspects of particle magnetism is the relationship between magnetic properties and particle size and shape. Since no uniform metal oxide dispersions were available, it was not possible to separate various magnetic phases as a function of particle size. This difficulty has now been overcome and Fig. 9 shows the change in magnetic susceptibility, χ, of spherical α-Fe_2O_3 particles as a function of their diameter, d, usinq the Faraday method; χ increases significantly when $d < 100$ nm. A practical consequence of this finding is the expectation that small hematite particles should be more easily removed by magnetic filtration than the larger ones. When $d > 100$ nm, the magnetic susceptibility is essentially equal to that of bulk α-Fe_2O_3. It was also shown that particles
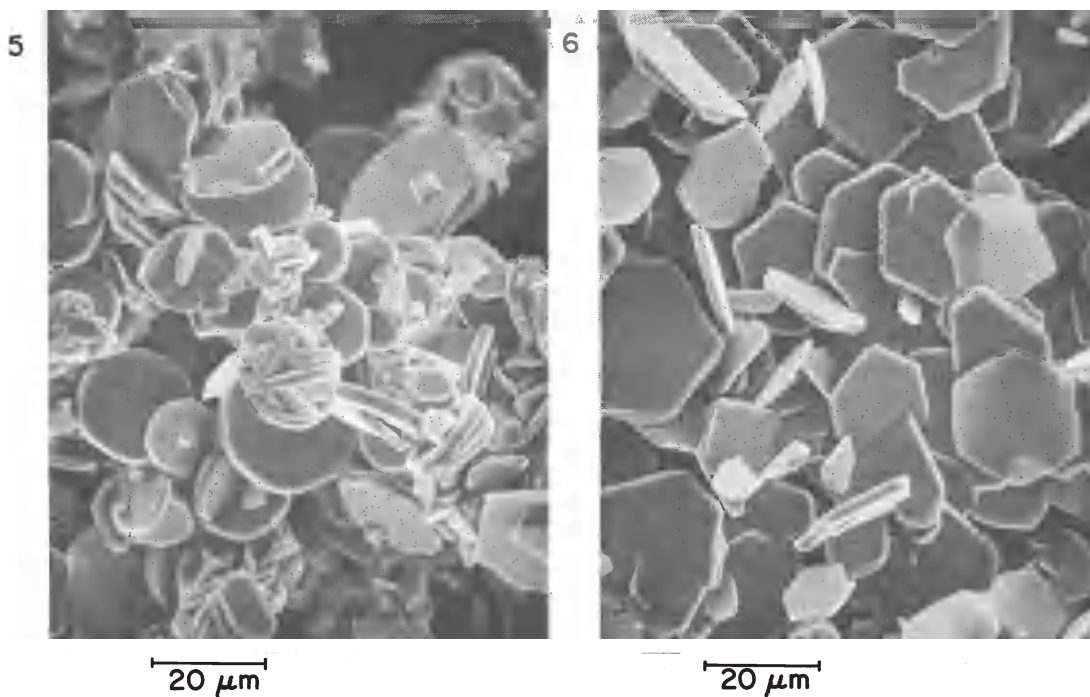
Fig. 5. Scanning electron micrograph of hematite (α-Fe$_2$O$_3$) particles obtained by aging for 1 hr at 250°C a solution 0.04 M in Fe(ClO$_4$)$_3$, 1.0 M in NaClO$_4$, 0.2 M in triethanolamine (TEA), 1.2 M in NaOH, and 0.5 M in H$_2$O$_2$.

Fig. 6. Scanning electron micrograph of hematite (α-Fe$_2$O$_3$) particles obtained by aging for 1 hr at 250°C a solution 0.04 M in Fe(NO$_3$)$_3$, 1.0 M in NaOOCCH$_3$, 0.2 M in TEA, and 1.2 M in NaOH.
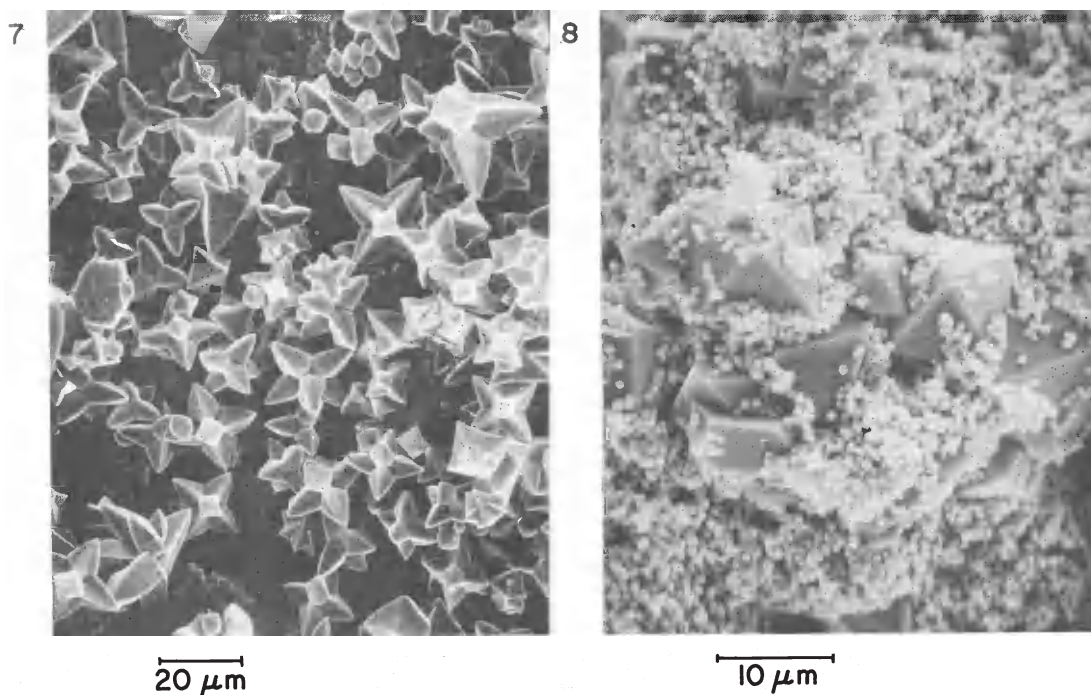
Fig. 7. Scanning electron micrograph of copper oxide particles obtained by aging for 70 min at 100°C a solution 0.04 M in Cu(NO$_3$)$_2$, 0.2 M in HEDTA, and 1.2 M in NaOH.

Fig. 8. Scanning electron micrograph of a mixture of α-Fe$_2$O$_3$ and Fe$_3$O$_4$ particles obtained by aging for 1 hr at 250°C a suspension of α-Fe$_2$O$_3$ particles (as illustrated in Fig. 2) in a solution 0.2 M in TEA, 1.2 M in NaOH, and 0.85 M in N$_2$H$_4$.
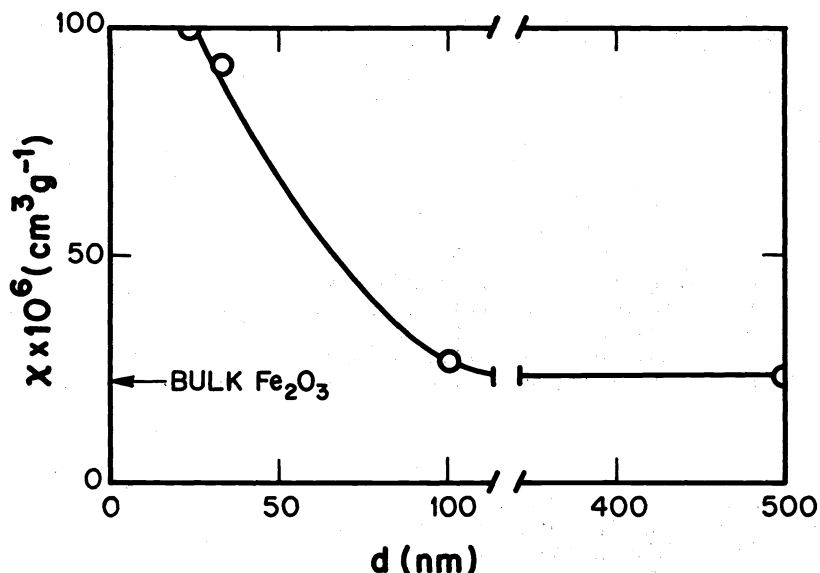
Fig. 9. Magnetic susceptibility of spherical hematite (α-Fe$_2$O$_3$) particles
as a function of their diameter.

of 100 nm in diameter are in the antiferromagnetic state as it was proposed earlier
(Ref. 11).

B. Electrokinetics

   Electrokinetic properties of the model corrosion products are important in explaining the
behavior of these materials as adsorbents or in interpretation of particle adhesion and
removal phenomena. The relationship of the electrokinetic behavior of the particles to their
size and shape has not been established with certainty, although it is expected that the ζ
potential should depend on these parameters. An attempt to use the uniform iron (hydrous)
oxide dispersions to resolve this question has not yet produced a reliable answer (Ref. 3).
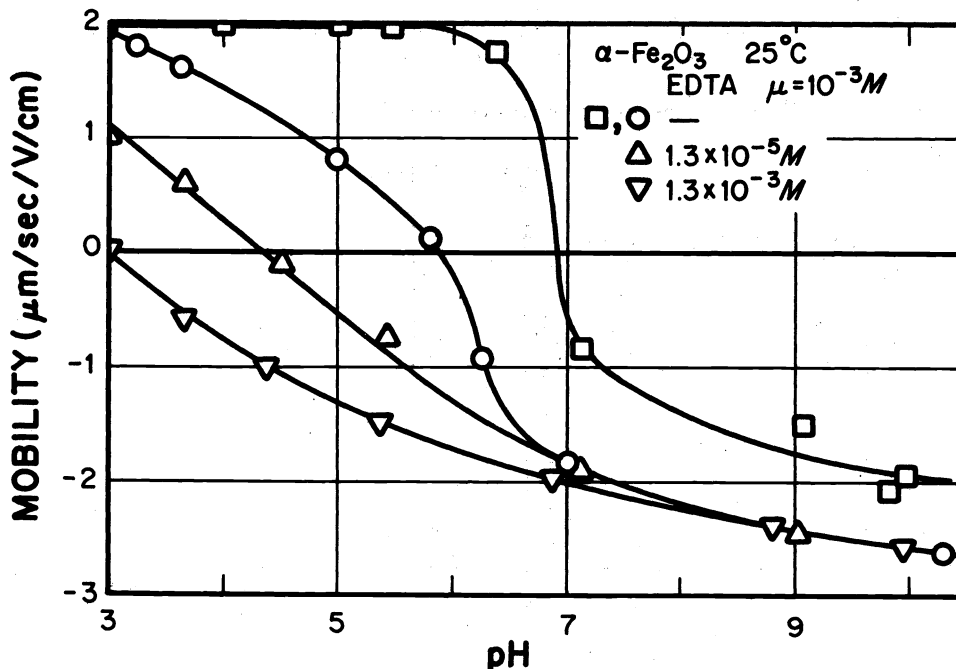   Electrokinetic data can indicate the adsorption of solute species on the suspended solids.

Fig. 10. Electrokinetic mobilities as a function of pH of spherical hema-
tite (α-Fe$_2$O$_3$) particles (260 nm in diameter) in the absence ($\bigcirc$,$\square$) and
in the presence of 1.3 x 10^{-5} M ($\triangle$) and 1.3 x 10^{-3} M (∇) EDTA. Squares
represent particles from which chloride ions were completely removed,
whereas circles are for particles which still contained Cl$^-$.

Figure 10 gives, as an example, the mobilities of spherical α-Fe$_2$O$_3$ particles as a function of pH. Two curves in the absence of any additives represent measurements which were carried out with a sol precipitated from solutions containing hydrochloric acid. Circles are for the systems as prepared with particles containing chloride ions, whereas squares give the mobilities for the same solids which were thoroughly rinsed with water until chloride ions were removed by leaching. Obviously, the contamination by this anion has a great effect on the surface charge characteristics; the isoelectric point (i.e.p.) is higher by approximately one unit for the completely purified sol and, furthermore, the mobility values are consistently higher over the range of pH < i.e.p. These results indicate the great sensitivity of the system towards the presence of nonconstituent ions.

The surface charge characteristics can be also affected by the adsorption of charged species. Two mobility curves given by triangles are for the same sol as shown by circles, except that EDTA was added to the system prior to measurements. Even a small amount of the chelating agent (1 x 10^{-5} M) has a pronounced effect on the particle charge. It is noteworthy that the adsorption of EDTA takes place on particles above their i.e.p. This observation indicates the coexistence of positively and negatively charged sites on the surface of α-Fe$_2$O$_3$.

C. Optics

The color of a dispersed system depends on the chemical composition of the solid (refractive index) and on the particle size and shape. As unbelievable as it may sound, there has been no dependable information on the refractive index of hematite, which is one of the most common pigments. By measuring the extinction and scattering of small monodispersed colloidal spheres of α-Fe$_2$O$_3$ it was possible to determine a reliable value for the absorption index of hematite for a broad range of wavelengths (Ref. 12). With this information the chromaticity of the model hematite pigment in dilute and concentrated systems was calculated and compared with the actual color appearance.

D. Stability

One of the fundamental problems of colloidal corrosion products is their stability in aqueous dispersions. In view of the fact that the resulting solids are metal (hydrous) oxides, their surface charge and stability in the suspended state is expected to be sensitive to pH. This statement should not imply that the charge is the only factor which may determine the state of such suspensions.

Figure 11 is a plot of relative scattering intensity of a monodispersed hematite sol as a function of pH. The high values designate stable sols whereas the low values denote coagulated and settled systems. A pronounced instability region is observed in the vicinity of the i.e.p. of the α-Fe$_2$O$_3$ particles. The coagulation at low and at high pH values is caused by high ionic strengths of the sols due to the addition of acid or base necessary to adjust the pH. As would be expected the presence of neutral electrolytes also affects the sol stability which is illustrated in Fig. 12. Sodium nitrate coagulates the positively
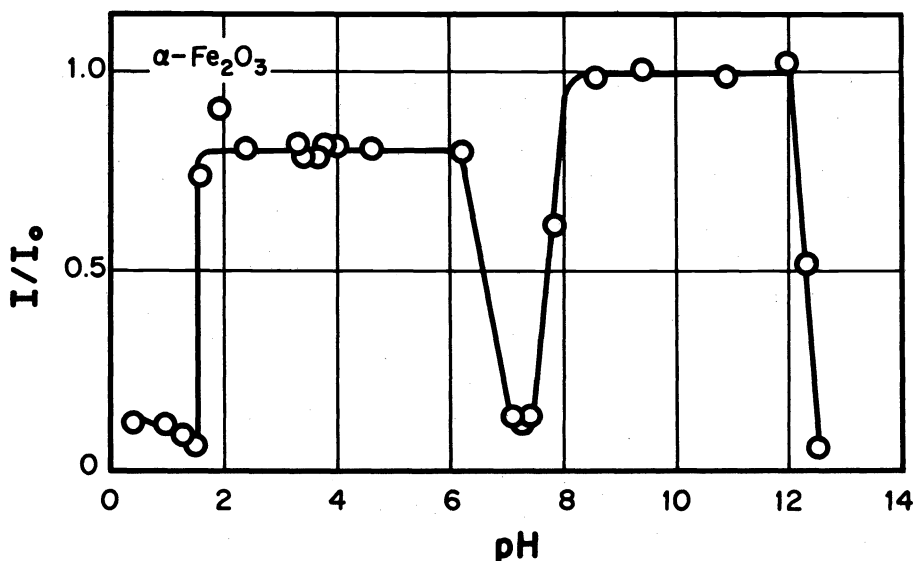

Fig. 11. Relative scattering intensities (I/I_0) as a function of pH of a hematite hydrosol (modal diameter $\sim$ 80 nm) having an isoelectric point of pH $\sim$ 7. Samples contained 6 x 10^9 spherical particles per cm^3. The pH was adjusted with either HNO$_3$ or NaOH. High values of I/I_0 represent stable sols.
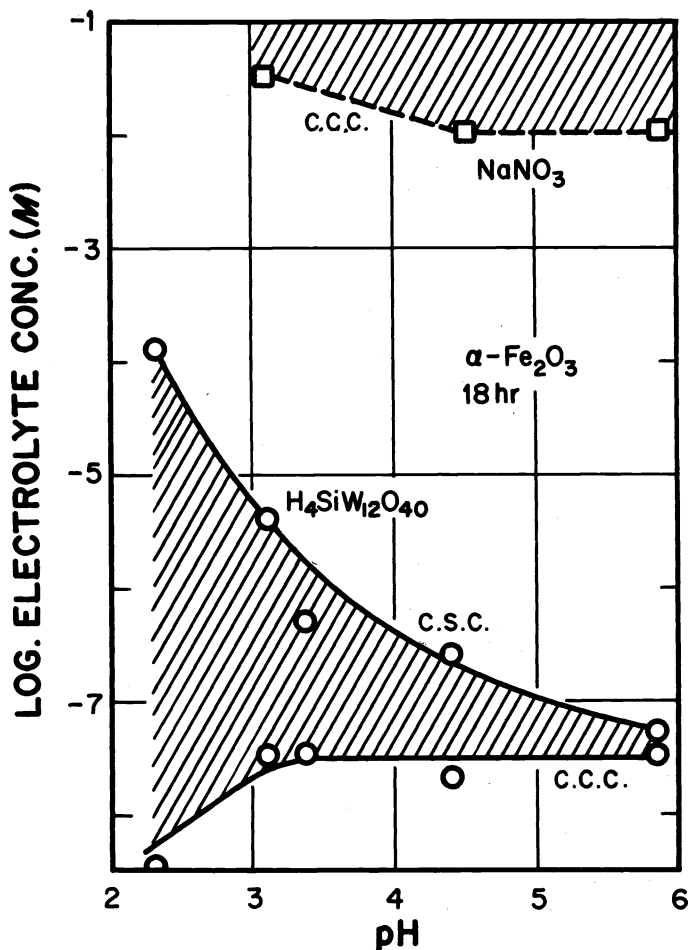
Fig. 12. Critical coagulation concentrations (c.c.c.) of $NaNO_3$ ($\square$) and
of $H_4SiW_{12}O_{40}$ (O) for the same hematite sol as in Fig. 11 as a function
of pH. Critical stabilization concentration due to charge reversal by
$H_4SiW_{12}O_{40}$ is indicated by c.s.c. Since the sol is positively charged,
anions act as coagulating or stabilizing agents. The instability region
is indicated by hatching.

charged hematite sol at a concentration typical for a monovalent counterion (NO_3^-).

The polyvalent tungstosilicate ion coagulates the same sol at an exceedingly low concen-
tration of $\sim 3 \times 10^{-8}$ M $SiW_{12}O_{40}^{4-}$ at pH between 3 and 6, and at an order of magnitude lower
concentration at pH of 2.3. The same anion restabilizes the sol at somewhat higher concen-
trations. This second stability region is due to the adsorption of the tungstosilicate ion
on hematite particles resulting in a change of the particle charge from positive to nega-
tive. The boundary is very sensitive to pH, at pH 5.8 the hematite sol is restabilized at
a concentration of $SiW_{12}O_{40}^{4-}$ as low as 5×10^{-8} M, while at pH 2.3 the effect is observed
at $\sim 1 \times 10^{-4}$ M tungstosilicic acid. This increase in anion concentration necessary to
restabilize the sol as the pH is lowered is caused by the higher charge on the particles and
by stepwise protonation of the tungstosilicate ion as the solution is acidified. Obviously,
the stability phenomena of colloidal corrosion products can be greatly affected by minute
quantities of counterions, which strongly interact with dispersed metal (hydrous) oxides.
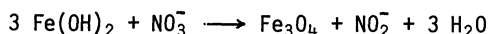
MECHANISMS OF PARTICLE FORMATION

In several cases it was possible to elucidate the mechanism of metal (hydrous) oxide for-
mation and growth. Chemical reactions preceding the particle nucleation are expected to
vary in each case, since complexes, which act as precursors to solid phase formation,
differ for every metal and depend on the pH, anions present, temperature, and other condi-
tions. The processes involved in the formation of spherical chromium hydroxide (Refs. 13
& 14) and titanium dioxide (Ref. 7) particles, as well as of crystalline ferric basic sul-
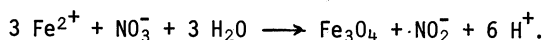fate colloids (Ref. 2) have been described in detail elsewhere and will not be repeated
here.

The interesting case of crystallization of uniform spherical magnetite particles (illus-
trated in Fig. 3) from ferrous hydroxide gels, was analyzed recently (Ref. 9), and it could

be shown that the larger spheres form on aggregation of very small primary magnetite particles. The latter appear on aging of the gel at an elevated temperature in the presence of the nitrate ion. The aggregates recrystallize and the resulting larger particles, trapped in the gel, grow further by attracting the primary particles that surround them. Once the vicinity of the large spheres is devoid of the small ones, no further growth can occur. The systems as described are generated only in excess of free Fe^{2+} ions.

The chemical processes which produce magnetite in the presence of the nitrate ion may involve the ferrous hydroxide gel and the free Fe^{2+} ions. They proceed along different pathways, such as

$$3 \ Fe(OH)_2 + NO_3^- \longrightarrow Fe_3O_4 + NO_2^- + 3 \ H_2O$$

and

$$3 \ Fe^{2+} + NO_3^- + 3 \ H_2O \longrightarrow Fe_3O_4 + NO_2^- + 6 \ H^+.$$

In the first case little change in pH should occur, whereas in the second case pH should decrease. Indeed, it was found that in course of crystallization of magnetite from $Fe(OH)_2$ gels, pH remained constant while the gel phase was still present, but the systems became more acidic afterwards. By using the radioactive isotope ^{59}Fe it was shown that the ferrous ions added to a $Fe(OH)_2$ suspension are readily incorporated into the gel and are subsequently detected in the magnetite (Ref. 9).

The above example indicates that rather involved mechanisms of metal (hydrous) oxide formation can be elucidated once well defined systems are available.

INTERACTIONS WITH COMPLEXING SOLUTES

The addition of complexing molecules, and particularly of chelating agents, to a solid/solution system may cause drastic changes in the interfacial properties, such as in the composition of the double layer, solvation and solubility of the solid substrate, adsorption and adhesion characteristics, and others. For this reason, the interactions of different complex forming species with a variety of solids have recently received increasing attention.

In this work the effects of a trimeric chelating agent, desferrioxamine (DFOB), which is a derivative of hydroxamic acid (HA)

$$\oplus H_3N-(CH_2)_5-N-C-(CH_2)_2-C-N-(CH_2)_5-N-C-(CH_2)_2-C-N-(CH_2)_5-N-C-CH_3$$
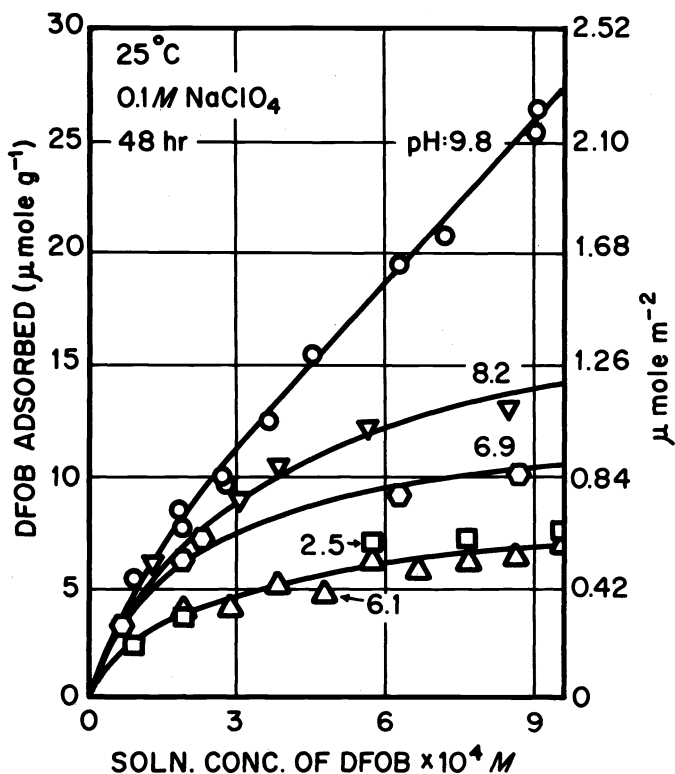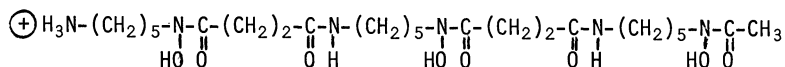

Fig. 13. The specific amounts of desferrioxamine (DFOB) adsorbed as a function of the concentration of DFOB added to a hematite sol (modal particle diameter 95 nm) after 48 hr of equilibration. Each curve is for a different pH value of the sol.
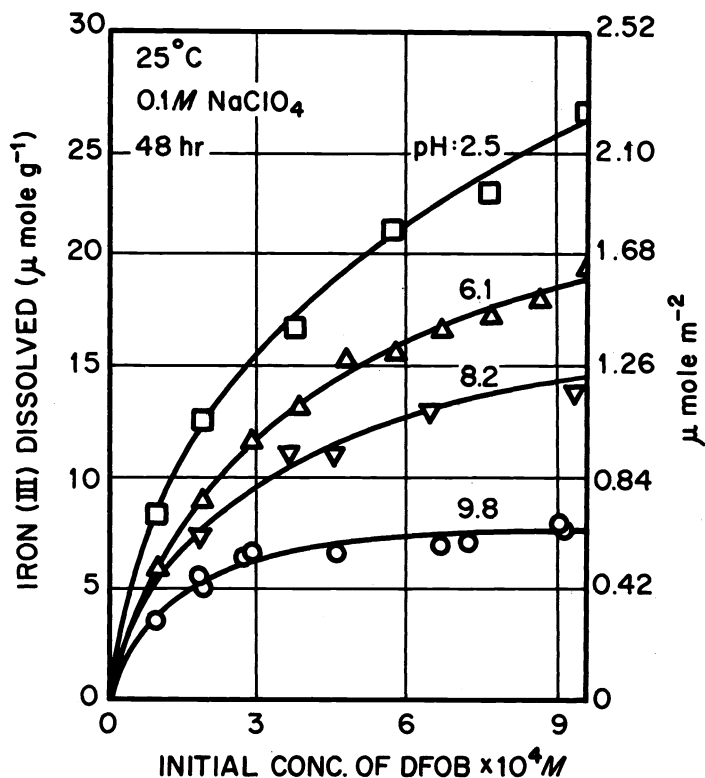
Fig. 14. The amount of iron(III) dissolved after 48 hr of equilibration
as a function of the DFOB concentration added to the same sol as in Fig. 13.
Each curve is for a different pH value of the sol.

on a monodispersed hematite sol are described and compared to interactions with a related
polymer (P-11) having 33 hydroxamic acid units (or 11 trimeric units).

Figure 13 gives several adsorption curves of DFOB on α-Fe$_2$O$_3$ particles, which show that
the uptake of the chelating species is relatively small and pH independent over the pH range
2.5 to 6, but increases rather sharply as the pH becomes higher. The data on dissolution of
hematite under the same conditions are presented in Fig. 14. The leaching of iron becomes
more pronounced as the concentration of DFOB increases and as the pH decreases.

The above observations can be understood if one considers the properties of the adsorbent
as well as the structure and the solution characteristics of the chelating molecule. For pH
< i.e.p. the particles and the DFOB are positively charged; thus, the adsorption must take
place via the chemical interaction of the HA ligands with the surface -FeOH and -FeOH$_2^+$
groups. The low adsorption density indicates a flat configuration of the chelating molecules
on the hematite surface. This arrangement could not account for the leaching of iron; thus,
a fraction of the molecules would have to be bound with one or more HA groups of the DFOB to
only one surface iron atom. It was found that the entire amount of the dissolved iron is
bound as a 3:1 (HA:Fe^{3+}) complex.

At pH > i.e.p. the adsorbed amount of DFOB at 48 hr of equilibration is increased, whereas
the leaching of iron(III) diminishes under the same conditions. At pH values between 7 and
8.4 the chelating molecules are positively charged whereas the hematite surface is negative.
Thus, the adsorption is enhanced by electrostatic attraction of the protonated amine groups
to the surface -FeO$^-$ species. This leads to a change in the orientation of the adsorbed
molecules with reduced likelihood of surface chelation. For a more detailed description of
these phenomena the reader is referred to the original paper (Ref. 15).

The adsorption isotherms at three pH values of the polymer (to be designated as P-11) on
the same hematite particles are given in Fig. 15. In acidic solutions the behavior is
typical for the uptake of macromolecules at solid/solution interfaces. The saturation
amount at pH 2.8 (2.3 mg m^{-2}) is an extraordinary high value which has not been reported
before for a polymer of a comparable molar mass. The corresponding area of $\sim$ 40Å^2 for a
trimer indicates a close packing of side chains. The decreasing uptake of P-11 at pH 9.0
is to be expected as the deprotonated HA groups of the polymer side chains are repelled by
the larger number of negative sites on α-Fe$_2$O$_3$.

No dissolution of hematite could be detected in the presence of the polymer P-11 which is
consistent with the above observations. The attachment of the side chains as bidentate
only, leaves the iron atom bound in the crystal lattice and no separation is expected. Ob-
viously, the chelate polymer is capable of forming a protective layer which stabilizes the
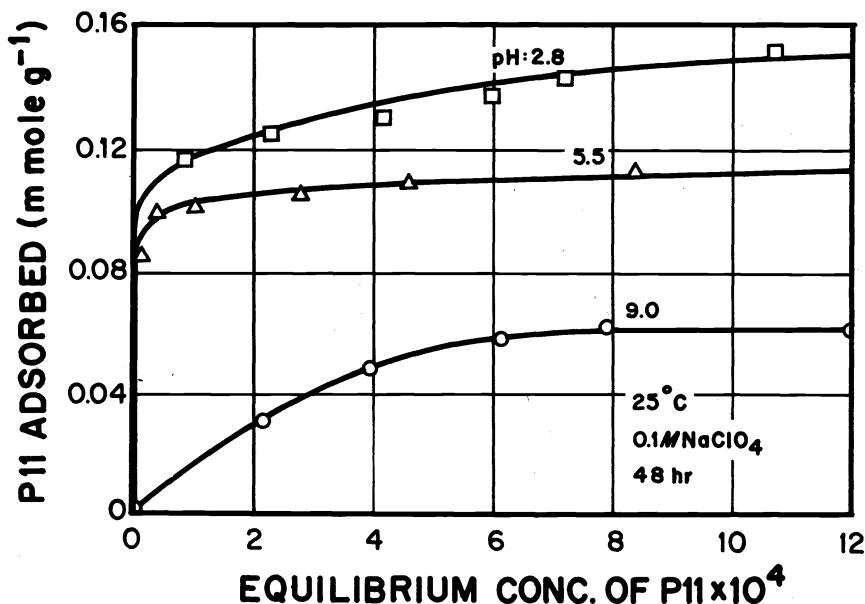hematite surface much more efficiently than the corresponding trimer molecules.

Fig. 15. The adsorption isotherms after 48 hr of equilibration for a hydroxamic acid polymer (P-11) for the same hematite sol as in Fig. 13 at three different pH values.

PARTICLE ADHESION AND DETACHMENT

Problems related to particle detachment and deposition are pertinent to the corrosion of metals. The protection of steel by corrosion films depends on the composition and structure of the metal oxide layers formed, as well as on their ability to adhere to the substrate. If the corrosion products are in particulate state or if the films are fractured and desorbed, the problems of deposition of the detached particles on other surfaces becomes significant.

Using the packed column method the problems related to particle adhesion and removal were studied with aqueous dispersions of colloidal spherical chromium hydroxide particles in contact with glass (Ref. 16) or steel (Ref. 17). It was shown that in these cases no chemical bonds existed between the particles and the substrate. The attempts to interpret the data in terms of the electrical double layer theory for the plate-sphere model offered only qualitative explanation of the observed phenomena. New results on interactions of spherical hematite particles with steel, to which an advanced theoretical treatment is applied, are illustrated here.

Figure 16 gives the fraction of α-Fe$_2$O$_3$ particles adsorbed on steel as a function of pH, along with the electrokinetic mobility curves for the adsorbent and adsorbate material. There is a narrow pH range over which the particle uptake is nearly quantitative; this range coincides with conditions yielding opposite charges on the two interacting solids.

The effect of the flow rate through the bed on the adhesion, as expressed in terms of single collector contact efficiency, σ, is given in Fig. 17. The quantity σ was derived by Levich and can be expressed as:

$$\sigma = 0.9 \left(\frac{kT}{nd_p^2 dv}\right)^{2/3}$$

where d_p is the diameter of the suspended particle, d the powder diameter used in the bed, v the flow rate of the sol through the bed, n the viscosity of the medium, k the Boltzmann constant, and T the absolute temperature. The solid line, calculated using the above equation for the conditions of the investigated system, shows that the obtained results are in a very good agreement with the model based on the diffusion mechanism. The Levich expression also explained reasonably well data taken at different temperatures (Ref. 18).

Desorption of the hematite particles from steel was followed by passing through the bed of steel beads, on which the colloidal spheres adhered, solutions of different pH and ionic strength. Again, it was found that the removal efficiency was very sensitive to pH of the rinsing solution (Fig. 18). Detachment took place over approximately two pH units and the particles remained adsorbed below and above this pH range. It is noteworthy that only a fraction of total number of adhered particles were able to escape. Furthermore, two different steels showed the same properties with respect to the desorption dependence on pH; however, the fraction removed differed considerably.

In view of the fact that no chemical bonding needs to be taken into account, the attractive forces of the van der Waals type and the repulsive double layer forces should account
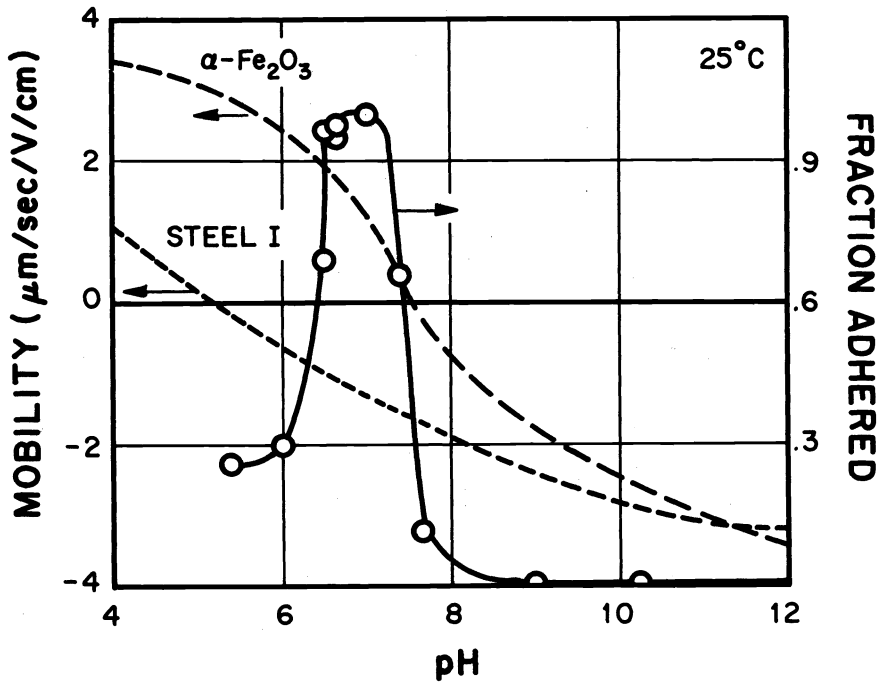
Fig. 16. Fraction of hematite (α-Fe$_2$O$_3$) particles deposited on steel as a function of pH at 25°C (solid line). In each case 50 cm^3 of the hematite sol (modal particle diameter of 170 nm) containing $\sim 10^8$ particles per cm^3 was passed through the bed at a flow rate of ~ 1 cm^3 min^{-1}. Electrophoretic mobilities of the particles and of steel are given by the dashed lines.
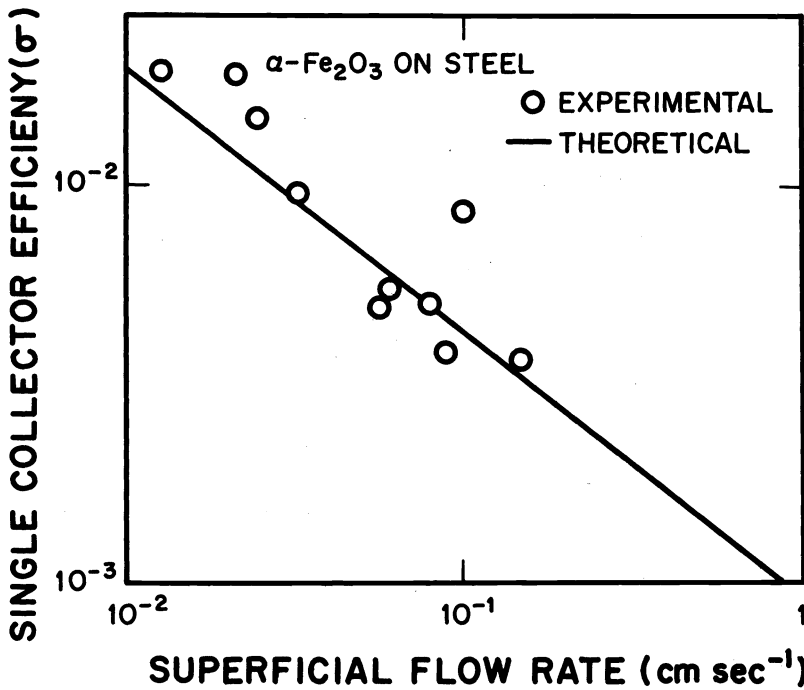

Fig. 17. Single collector efficiency, σ, as a function of the superficial flow rate for the same system described in Fig. 16. The solid line is the theoretical function calculated from Levich's expression.
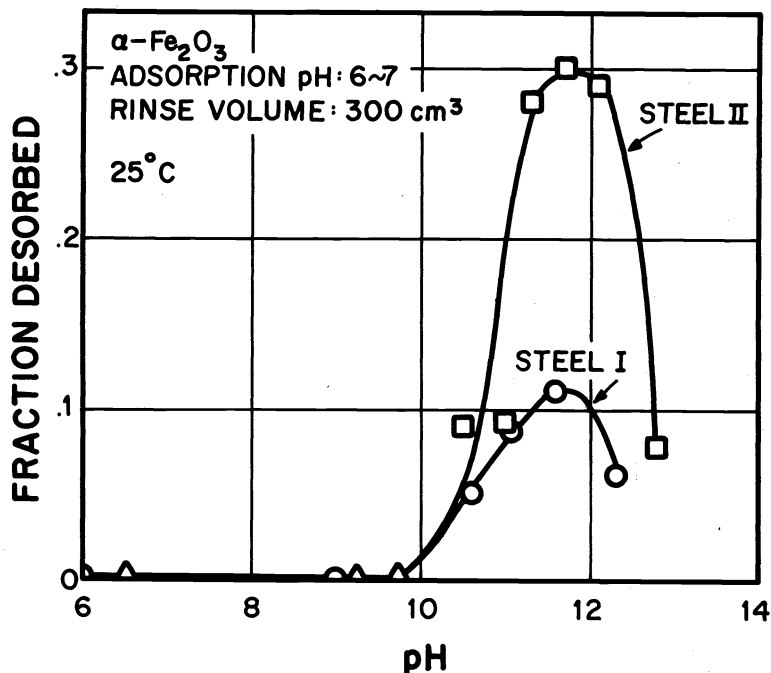
Fig. 18. Fraction of hematite particles desorbed from two different steel
samples on continuous elution with rinse solutions of different pH. The
total rinse volume was 300 cm³. The number of particles adsorbed at pH
6-7 was $\sim 10^9$.

for the desorption behavior of the studied systems. Once the particles are on the surface,
the probability of their escape depends on the energy barriers the particles have to sur-
mount. To calculate the van der Waals potential energy, the known expression for the inter-
action of unlike spheres with appropriate values of Hamaker constants was used.

The double layer potential energy was estimated from the expression of Hogg, Healy, and
Fuerstenau (HHF) (Ref. 19) and from the equation which treats the problem of unequal spheres
by employing the Poisson-Boltzmann equation in its two-dimensional form (BMRF) (Ref. 20).
Figure 19 gives the total interaction energies for four different pH values as they apply to
systems shown in Fig. 18. It is evident that $\phi(x)/kT$ as calculated from the HHF model is
much too high to account for the observed effects. The corresponding energies based on the
BMRF expression are quite reasonable, and they explain the properties of the systems at
different pH values. Thus, at pH 12.8 attraction prevails over all separations and indeed
no particle desorption is detected. At pH 10 the repulsion barrier extends far into the
solution phase which makes the desorption of the particles unlikely. At intermediate pH
values the relatively low potential barrier allows for a finite probability of particle es-
cape, as found experimentally. It should be noted that the separation of the adhered par-
ticle from the surface will determine the actual amount of the activation energy which the
particles must surmount in order to diffuse away.

The finding that only a fraction of adsorbed particles is removed can be explained by the
irregularities of the steel surface. Scanning electron micrographs have shown that the
latter abounds in well pronounced crevices. The force acting on the particles trapped in
these channels is different than calculated for the plate/sphere geometry. Thus, the total
energies as evaluated cannot explain the behavior of embedded particles.

The examples given here show that the fundamental aspects of particle adhesion and de-
sorption can be accounted for if the refined treatment of the double layer is taken into
consideration as long as no chemical or other types of energies are involved. Indeed,
introducing a magnetic field around the packed column changes the entire adsorption/de-
sorption behavior of a given system. Similarly, chemical modifications of the surface
properties either of the bed powder or of the particles can also alter the adhesion
and particle removal characteristics of the otherwise identical systems.

CONCLUDING REMARKS

In the preceding sections a few problems of interest in the study of corrosion of metals
have been described. It is obvious that the discussed phenomena deal with fundamental as-
pects of colloid and interface science. The work so far carried out may be considered just
as the beginning of a program in an important area of application which offers a variety of
challenging problems. Indeed, a considerable effort by workers in this discipline will be
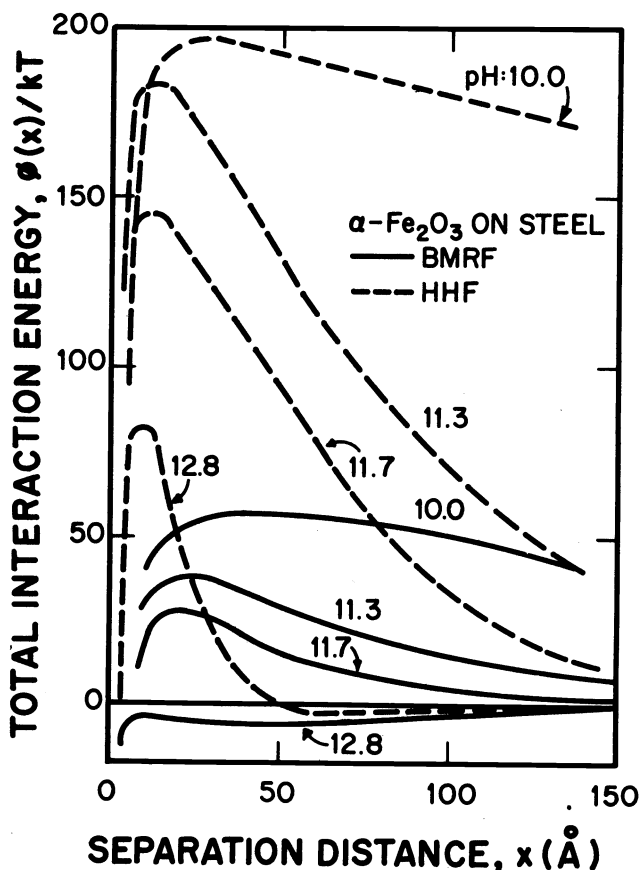needed if various corrosion processes are to be elucidated.

Fig. 19. Calculated total potential energies, $\phi(x)/kT$ as a function of
separation using the expression of Barouch, Matijević, Ring, and Finlan
(————, Ref. 20), and of Hogg, Healy, and Fuerstenau (— — —, Ref. 19),
for the system hematite on steel at four different pH values.

REFERENCES

1.   E. Matijević, R. S. Sapieszko and J. B. Melville, J. Colloid Interface Sci. 50,
     (1975).
2.   R. S. Sapieszko, R. C. Patel and E. Matijević, J. Phys. Chem. 81, 1061 (1977).
3.   E. Matijević and P. Scheiner, J. Colloid Interface Sci. 63, 509 (1978).
4.   R. Brace and E. Matijević, J. Inorg. Nucl. Chem. 35, 3691 (1973).
5.   R. Demchak and E. Matijević, J. Colloid Interface Sci. 31, 257 (1969).
6.   E. Matijević et al., J. Colloid Interface Sci. 36, 273 (1971).
7.   E. Matijević, M. Budnik and L. Meites, J. Colloid Interface Sci. 61, 302 (1977).
8.   P. McFadyen and E. Matijević, J. Colloid Interface Sci. 44, 95 (1973).
9.   T. Sugimoto and E. Matijević, J. Colloid Interface Sci. (in press).
10. R. S. Sapieszko and E. Matijević, J. Colloid Interface Sci. (submitted).
11. Yu. F. Krupyanskii and I. P. Suzdalev, Sov. Phys. - JETP 38, 859 (1974).
12. M. Kerker, P. Scheiner, D. D. Cooke and J. P. Kratohvil, J. Colloid Interface Sci.
     (in press).

13. A. Bell and E. Matijević, J. Inorg. Nucl. Chem. 37, 907 (1975).
14. A. Bell and E. Matijević, J. Phys. Chem. 78, 2621 (1974).
15. J. Eisenlauer and E. Matijević, J. Colloid Interface Sci. (submitted).
16. J. E. Kolakowski and E. Matijević, J. Chem. Soc., Faraday Trans. I, 75, 65 (1979).
17. R. Kuo and E. Matijević, J. Chem. Soc., Faraday Trans. I (in press).
18. R. Kuo and E. Matijević, J. Colloid Interface Sci. (submitted).
19. R. Hogg, T. W. Healy and D. W. Fuerstenau, Trans. Faraday Soc. 62, 1638 (1966).
20. E. Barouch, E. Matijević, T. A. Ring and J. M. Finlan, J. Colloid Interface Sci. 67, 1
     (1978); 70, 400 (1979).